



Research Article

Thermodynamic analysis of a solar-driven vapor compression re-refrigeration system using R1234ze for cooling applications in Ghardaïa region (Southern Algeria)

Ahmed SELLOUM¹, Zakaria TRIKI^{1,*}, Younes CHIBA¹

¹Laboratory of Biomaterials and Transport Phenomena, University of Medea, Medea 26000, Algeria

ARTICLE INFO

Article history

Received: 21 June 2023

Accepted: 04 October 2023

Keywords:

Solar Energy; Vapor Compression Refrigeration; Low GWP Refrigerant; Cooling Applications; Performance; Comparison

ABSTRACT

This study presents a thermodynamic analysis of a solar-driven vapor compression refrigeration (VCR) system designed for use in the region of Ghardaïa (Southern Algeria) which is located in a desert with a semi-arid climate where the demand for cooling is high, and the solar radiation is abundant. Two working fluids are tested and compared, the HFC high GWP going to phased out, R134a and the low GWP, HFO refrigerant recently introduced R1234ze. The performance of the solar VCR system was evaluated using a numerical model developed in MATLAB software, based on thermodynamic properties of R1234ze and R134a refrigerants. The results showed that coefficient of performance (COP) and thermodynamic efficiency of the solar VCR system increased with decreasing ambient temperature due to the increase in the compressor power consumption. The COP during the 21st day of July month is obtained in the range of 4.37–5.77 for R1234ze refrigerant which are close and more than 90% of the maximum COP value, while it is in the range of 2.56–3.17 for R134a fluid. The lowest COP values are found around noon hours during 12:00 AM and 15:00 PM. In addition, the greatest amount of the PV power production for R134a and R1234ze refrigerants occurs in the middle of the day (12:00 PM) as 2.8 and 1.6 kWh, respectively.

Cite this article as: Selloum A, Triki Z, Chiba Y. Thermodynamic analysis of a solar-driven vapor compression re-refrigeration system using R1234ze for cooling applications in Ghardaïa region (Southern Algeria). J Ther Eng 2024;10(1):130–141.

INTRODUCTION

Solar-based cooling is an indispensable domain within the realm of renewable energy and has garnered noteworthy accomplishments. Its significance arises from the heightened requirement for cooling during periods of intensified solar radiation, which often aligns with hotter climates.

Furthermore, solar cooling stands out for its environmentally conscious nature, given its absence of greenhouse gas emissions and its contribution to curbing reliance on fossil fuels. Notably, it offers cost-effective advantages by lowering energy expenditures and entailing minimal maintenance costs. Another notable advantage lies in its applicability to

*Corresponding author.

*E-mail address: triki.zakaria@univ-medea.dz

This paper was recommended for publication in revised form by Ahmet Selim Dalkılıç



remote regions lacking easy access to electricity, rendering it a viable solution for off-grid scenarios [1].

Solar cooling systems can be broadly categorized into two primary types: solar thermal cooling systems and photovoltaic (PV) cooling systems. Solar thermal systems directly utilize solar radiation to expose the refrigerant, eliminating the need for electrical power. Conversely, PV cooling systems harness electricity generated by PV modules to drive their operations. Within the realm of thermal cooling systems, there exist four distinct categories: solar adsorption, absorption, ejector, and desiccant systems.

On the other hand, PV-based solar cooling systems can be classified as either thermoelectric refrigeration systems or PV compression refrigeration systems. Among these, PV solar vapor compression refrigeration (VCR) systems prevail as the most commonly utilized and commercially accessible options. Notably, they have found practical applications in cold storage and the preservation of vaccines in rural areas [2–4].

Numerous experiments have been conducted to evaluate the effectiveness of vapor compression solar cooling systems, encompassing both alternating current (AC) and direct current (DC) variants [5–17]. In addition, various researchers have undertaken theoretical investigations into solar cooling systems using PV technology [18–26]. One particular focus in recent years has been on low global warming potential (GWP) refrigerants, with studies exploring the utilization of refrigerant mixtures with low GWP values to enhance the performance of vapor refrigeration systems. Hydro-Fluoro-Olefin (HFO) refrigerants like R1234yf and R1234ze have emerged as promising alternatives to Hydro-Fluoro-Carbon (HFC) refrigerants due to their reduced GWP values.

Mota Babiloni et al. [27] compiled relevant research on R1234ze, encompassing investigations into its thermophysical and compatibility properties, heat transfer and pressure drop characteristics, and the performance of vapor compression systems incorporating this refrigerant. Other studies have assessed the viability of R1234ze and HFO1234yf as alternatives to HFC-134a, analyzed vapor compression refrigeration (VCR) systems employing different evaporators, and compared the performance of various vapor compression configurations utilizing low GWP refrigerants.

In a study by Ben Jemaa et al. [28], an exergy analysis was conducted on an air-cooled vapor compression chilled water system utilizing R1234ze, with findings indicating no significant differences in energy and exergy efficiencies when compared to R134a.

Rajendran Prabakaran et al. [29] conducted a comprehensive examination of the thermodynamic performance of an automobile air conditioning (AAC) system at three distinct vehicle speed conditions, employing R134a, R1234yf, and a 50/50 mixture of R1234yf and R134a. Their findings indicated that the performance of the R1234yf/R134a mixture closely resembled that of R134a within the AAC unit. However, they proposed utilizing a 90/10 R1234yf/R134a

mixture to adhere to environmental protocols (GWP <150) without necessitating component modifications.

Toualbi et al. [30] investigated the energy performance of a vapor compression refrigeration cycle employing low GWP fluids (R1234yf and R1234ze) and compared it to high GWP fluids. The study revealed that R1234ze exhibited a superior coefficient of performance (COP) of 3.14, which closely approached that of R134a (3.17).

More recently, Shamkar Prasad et al. [31] carried out both experimental and simulation investigations to explore various refrigerants and blends as potential replacements for R134a in vapor compression refrigeration systems. The researchers analyzed heat transfer parameters and predicted the performance of low-GWP refrigerants across the HFO and HFC categories through energy and exergy analyses, considering commercial refrigerants such as R134a.

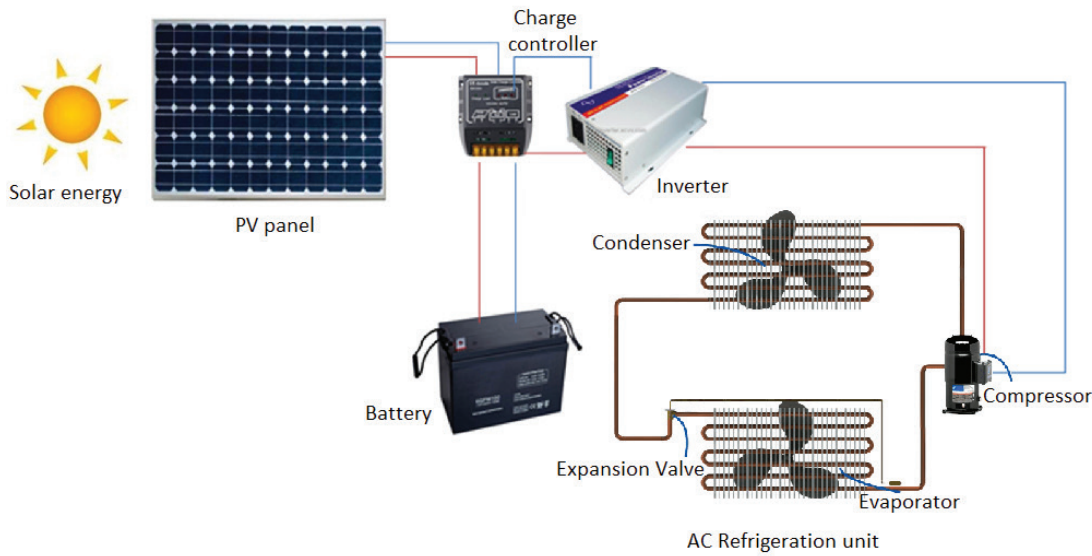
Despite the various studies found in the literature, there seems to be a lack of comprehensive thermodynamic analysis for solar-driven vapor compression refrigeration system using R1234ze fluid as an alternative of R134 refrigerant for cooling applications. The mentioned gaps in the existing literature have been addressed by the presented study. In addition, the use of solar energy to power refrigeration systems is an emerging area of research and innovation, especially in regions with abundant sunlight. The aim of this paper is to evaluate the thermodynamic performance of a solar-driven VCR system in the Ghardaïa region (southern Algeria) located in the Sahara Desert with hot and arid climate zone, which makes it an ideal location for the use of solar energy for cooling applications. The traditional method of cooling in this region is through the use of evaporative coolers, which are not very efficient and consume a significant amount of water. The use of a solar-driven VCR systems can provide a more energy-efficient and environmentally friendly cooling solution for this region. Two working fluids are studied and compared, the HFC high GWP going to be phased out, R134a and the low GWP, HFO refrigerant recently introduced R1234ze.

MATERIALS AND METHODS

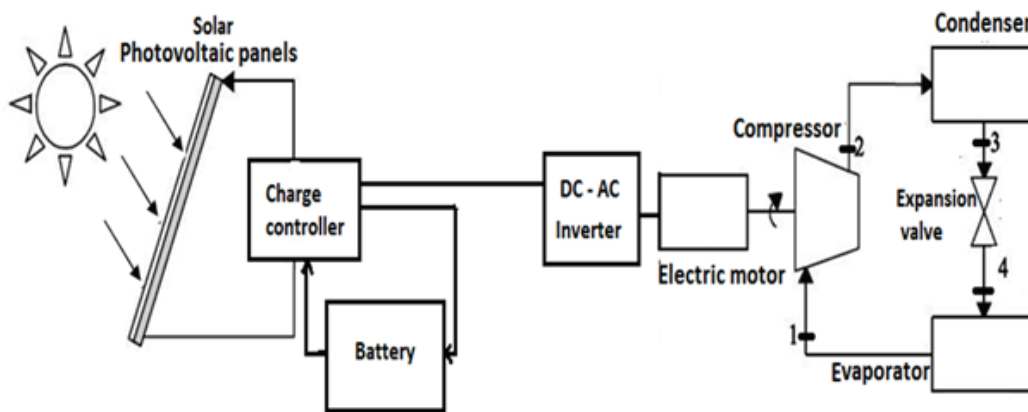
System Description

The diagram in Figure 1 illustrates the key components of the solar VCR system under investigation. The system consists mainly of an AC refrigeration unit, a charge controller that prevents the battery from being over charged or deep-discharged, a DC-AC inverter which converts direct current from the solar PV panel or the battery into alternating current that can be fed to a conventional AC compressor, a battery to store and supply energy when the sun is not available and a PV generator which supplies power to the refrigeration unit and charges the battery with excess energy.

The compressor plays a crucial role in compressing the refrigerant gas (1) to form a high-pressure and high



(a)



(b)

Figure 1. Schematic diagram of the solar PV assisted cooling system.

temperature gas. This high-pressure gas (2) is then directed to the condenser, where it dissipates heat and undergoes condensation, transforming into a high-pressure and high-temperature-liquid. Subsequently, the high-pressure and high-temperature liquid (3) proceeds through a throttling mechanism, such as an expansion valve, experiencing a reduction in pressure and transforming into a low-pressure and low-temperature liquid. This low-pressure and low-temperature liquid (4) is then introduced into the evaporator, where it absorbs heat from its surroundings and transitions into a low-pressure and low-temperature gas. The resulting low-pressure and low-temperature gas is subsequently routed back to the compressor, initiating the cycle anew. A pressure-enthalpy diagram depicting the vapor compression cycle is provided in Figure 2.

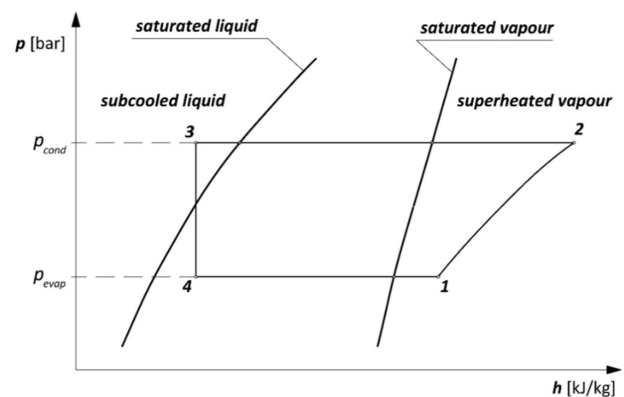


Figure 2. Pressure-enthalpy diagram of a vapor compression refrigeration cycle.

Site Description

The city of Ghardaia, situated in the southern region of Algeria at latitude 32.26° N and longitude 03.46° E, experiences a hot and arid climate characterized by minimal annual rainfall. In this study, climatic data were obtained from the meteorological station located at the Renewable Energy Applied Research Unit (URAER) in Ghardaia [32]. Figure 3 illustrates the monthly variations in ambient temperature and solar global radiation for the Ghardaia region. It is evident that February registers the lowest temperatures, averaging at 23.3°C, while June represents the warmest month with an average temperature of 33.7°C. The annual average ambient temperature hovers around 25°C. Regarding solar radiation, the highest monthly value of 205 kWh/m² occurs in July, making it the selected month for the ongoing research.

Working Fluids

R134a, categorized as a hydrofluorocarbon (HFC), is known for its absence of Ozone Depletion Potential (ODP). Nevertheless, the environmental impact of a working fluid extends beyond the depletion of the stratospheric ozone layer when it is released into the atmosphere. While HFCs do not harm the earth’s stratospheric ozone layer, certain HFCs with high Global Warming Potential (GWP) can significantly contribute to climate change. Under the Kyoto Protocol in 1997 [33], HFCs were classified as greenhouse gases and efforts have been made in many developed countries to reduce their emissions. Consequently, there is a search for alternative substances to replace high GWP

HFCs, including R134a, which possesses a GWP of 1430 (as shown in Table 1).

Hence, the utilization of HFCs with a Global Warming Potential (GWP) exceeding 150 in HVAC and VCR systems is regulated by European Regulation No. 2006/40/EC and No. 517/2014 [34,35]. As a result, R134a is slated for prohibition in the near future, prompting the search for viable alternatives such as the hydro-fluoro-olefin (HFO) R1234ze(E). This particular HFO shows promise due to its significantly lower GWP and shorter atmospheric lifetime (17 days for R1234ze compared to 13.8 years for R134a) [36]. However, despite its environmentally friendly characteristics, some drawbacks have been identified, including its slight flammability and potential negative impact on overall performance, particularly in terms of vapor compression efficiency [37].

Table 1. Refrigerant properties of R134a and R1234ze [38,39]

Property	R134a	R1234ze
ASHRAE safety classification	A1	A2L
ODP (Ozone Depletion Potential)	0	0
GWP (Global Warming Potential)	1430	7
Critical temperature [K]	247.08	253.88
Critical pressure [kPa]	4059.28	3623.90
Specific heat ratio (γ)	1.12	1.101
Vapor density [kg·m ⁻³]	14.35	11.65
Liquid density [kg·m ⁻³]	1295	1240
Latent heat of vaporization [kJ·kg ⁻¹]	198.72	184.28

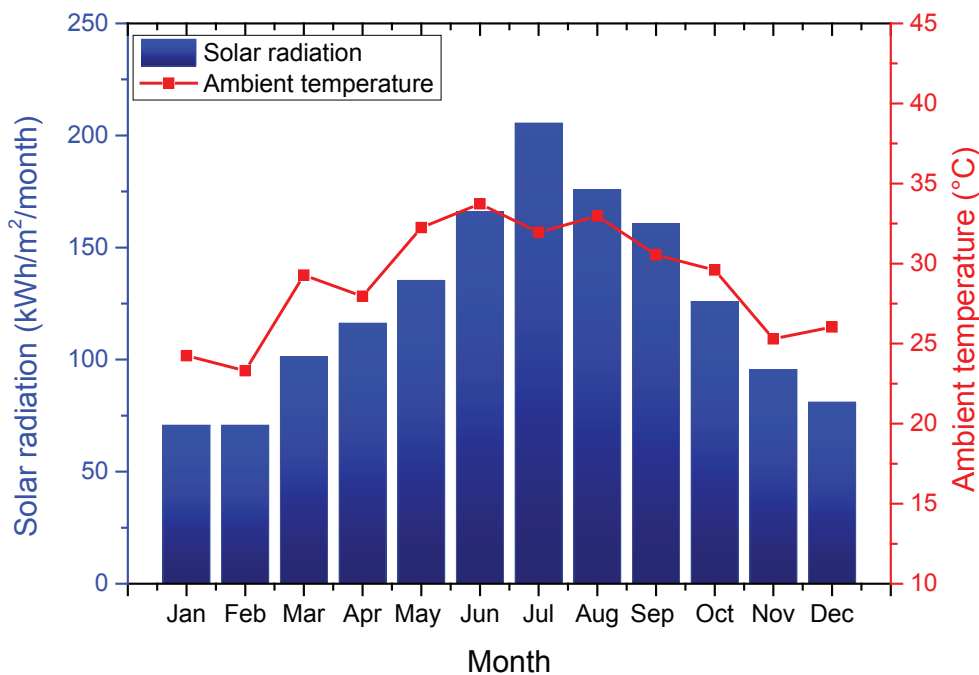


Figure 3. Monthly solar radiation and average daily ambient temperature (Ghardaia site) [32].

Thermodynamic Analysis

Vapor-compression refrigeration system

To model the solar vapor compression refrigeration system, the principles of mass conservation and the first law of thermodynamics are utilized for every cycle component, considering the following assumptions:

- Steady-state operation
- Reversible heat transfer
- Polytropic compression
- Negligible variations in kinetic and potential energy
- Insignificant pressure drops
- Consistent cooling capacity

When considering a control volume encompassing the refrigerant side of the evaporator, the refrigerant's mass flow rate (\dot{m}) is defined as follows [40]:

$$\dot{m} = \frac{Q_e}{(h_1 - h_4)} \quad (1)$$

Where: h_1 and h_4 are the specific enthalpies at states (1) and (4), respectively (kJ/kg).

Q_e is the heat transfer rate, which is referred to as the cooling capacity (kW).

The compressor power consumption is defined as follows [41]:

$$W = \frac{\dot{m}(h_2 - h_1)}{\eta_e \cdot \eta_b \cdot \eta_m} \quad (2)$$

Where: h_2 is the specific enthalpy at state (2) (kJ/kg).

η_e , η_b , and η_m are respectively called as electric motor efficiency, belt transmission efficiency and compressor mechanic efficiency.

Knowing the compressor exit temperature, the specific enthalpy (h_2) at the exit of the compressor can be determined. The discharge temperature based on the polytropic is calculated as follows [42]:

$$T_2 = T_1 \left(\frac{P_c}{P_e} \right)^{\gamma-1/\gamma} \quad (3)$$

Where: P_c and P_e are the condenser and evaporator pressures, respectively (bar).

γ is the polytropic exponent (defined as the ratio between the specific heat at constant pressure and constant volume, C_p/C_v).

For a control volume enclosing the refrigerant side of the condenser, the rate of heat transfer (Q_c) from the refrigerant per unit mass of refrigerant is as follows:

$$Q_c = \dot{m}(h_2 - h_3) \quad (4)$$

The process in expansion valve is usually modeled as a throttling process for which:

$$h_3 = h_4 \quad (5)$$

where h_3 is the specific enthalpy at state (3) (kJ/kg).

Coefficient of the performance (COP) is defined as the cooling power, Q_e divided by the work input, W :

$$\text{COP} = \frac{Q_e}{W} \quad (6)$$

Heat losses are a common occurrence in cooling systems, leading to a deviation between the actual coefficient of performance (COP) and its theoretical maximum COP. The thermodynamic efficiency refers to the ratio between the COP of the actual refrigeration system and the COP of a reversible refrigeration system operating within the same temperature range:

$$\eta_{th} = \frac{\text{COP}}{\text{COP}_{max}} \quad (7)$$

Where: COP_{max} is the maximum coefficient of performance of the refrigeration system which depends mainly on its operating temperatures.

$$\text{COP}_{max} = \frac{T_c}{T_c - T_e} \quad (8)$$

Equations for calculations of the thermodynamic properties of R134a and R1234ze refrigerants are presented in [43] and [44], respectively. The developed correlations are a function of one variable for the state of saturation and two variables for the subcooled liquid and superheated vapor regions.

Solar PV panel

The calculation of PV power production involves the utilization of the solar electric panel's efficiency, denoted as η_{PV} , and the solar radiation input, represented as Q_s [45].

$$W_{PV} = \eta_{PV} \cdot Q_s \quad (9)$$

The generation of solar radiation from the surface area of the panel and the overall efficiency of a cooling system assisted by solar PV are defined as follows:

$$Q_s = A \cdot I \quad (10)$$

$$\eta_s = \eta_{PV} \cdot \text{COP} \cdot \frac{Q_c}{Q_s} \quad (11)$$

Where: A is the solar cell or panel surface area (m^2) and I is solar radiation (kW/m^2).

In the solar vapor compression refrigeration system, the objective is to fulfill the compressor's power requirements through electricity generated by solar PV panels.

Consequently, it is necessary to ensure an adequate number of PV panels with appropriate characteristics to meet the system’s energy demand entirely. The daily cumulative power consumption of the compressor and the daily cumulative power production of the PV panels can be calculated using the following expressions:

$$W_T = \sum_{i=1}^k W_i \quad (k = 1, 2, \dots, 24) \quad (12)$$

$$(W_{PV})_T = \sum_{i=1}^k (W_{PV})_i \quad (k = 1, 2, \dots, 24) \quad (13)$$

Where: k is the hour of the day.

The required PV panel area can be determined by using the following equation:

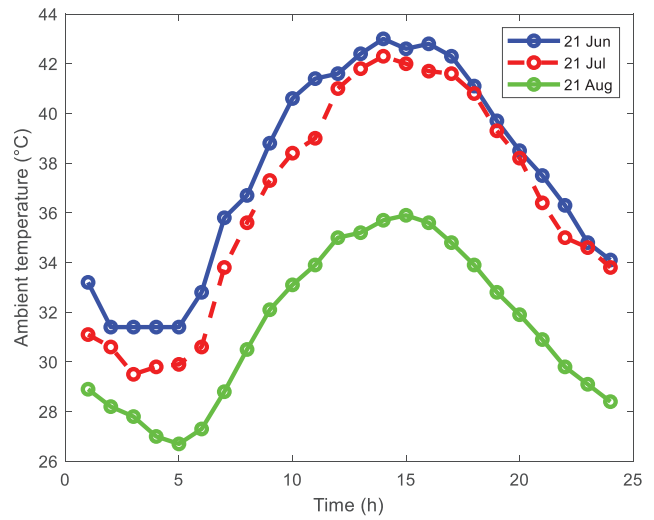
$$A = \frac{W_T}{\eta_{PV} \cdot I_T} \quad (14)$$

Here: I_T is the daily total solar radiation ($\text{kWh}/\text{m}^2/\text{day}$).

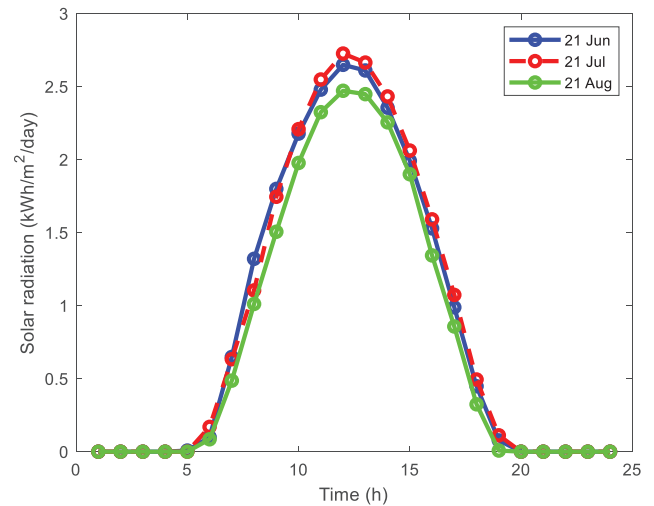
The fundamental operational parameters, derived from previous studies, which determine the performance of the cycle, are provided in Table 2.

RESULTS AND DISCUSSION

Figure 4 illustrates the measured hourly average variations of solar radiation and ambient temperature for the Ghardaia region during the 21st day of June, July, and August. As depicted in Figure 4(a), the hourly ambient temperature experiences a significant range of variation throughout the day, with the highest average temperature occurring in June and July, and the lowest in August. Figure 4(b) demonstrates that solar irradiation increases with sunlight, reaching its peak values at noon. Subsequently, it gradually decreases during the evening hours when the



(a) Ambient temperature



(b) Solar radiation

Figure 4. Hourly mean variation of solar radiation and ambient temperature (Ghardaia site).

solar energy’s influence diminishes, and there is no solar energy effect between 8:00 PM and 4:00 AM. Moreover, the hourly solar radiation values in July surpass those of other months. The maximum solar radiation value, with a magnitude of $2.726 \text{ kWh}/\text{m}^2$, is recorded at 12:00 PM on June 21. Comparing the maximum values of ambient air temperature and solar radiation, it is observed that the maximum atmospheric temperature occurs between 1:00 PM and 2:00 PM, whereas the maximum solar radiation is registered between 12:00 PM and 1:00 PM.

Figure 5 presents a comparison of the hourly mass flow rates for both refrigerants on July 21. The calculation results indicate that the mass flow rate of R1234ze is noticeably higher than that of R134a. This difference is primarily due to R134a having a higher boiling point and heat of vaporization compared to R1234ze at a given temperature.

Table 2. Operating parameters

Parameter	Value
Nominal cooling capacity	2 kW
Evaporating Temperature	0°C
Condenser temperature approach	15 K
Superheat	5 K
Subcooling	5 K
Electric motor efficiency	95%
Belt transmission efficiency	100% (direct transmission)
Compressor mechanic efficiency	80%
PV panel efficiency	20%

Consequently, R134a exhibits a greater cooling capacity, as depicted in Figure 6, meaning that a lower mass flow rate of R134a is typically required to achieve the same cooling effect as R1234ze. The lower cooling capacity for R1234ze refrigerant compared to R134a, with an average reduction equal to 10% is comparable with the findings of other experimental works present in the literature [46–48].

Furthermore, R134a has a lower specific volume and higher density in comparison to R1234ze. This implies that a smaller mass of R134a can occupy the same volume as a larger mass of R1234ze, resulting in a reduced mass flow rate requirement for R134a. Additionally, the mass flow rate experiences variations throughout the day. As the ambient temperature rises, the heat load on the system increases, necessitating a higher mass flow rate of refrigerant to maintain the desired cooling capacity.

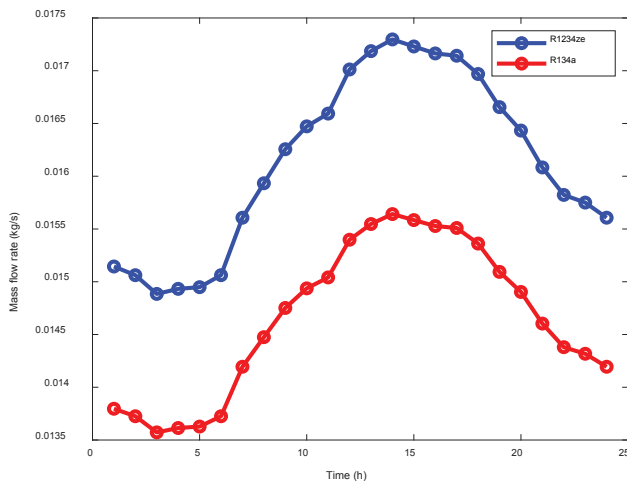


Figure 5. Hourly variation of mass flow rate (Ghardaia site).

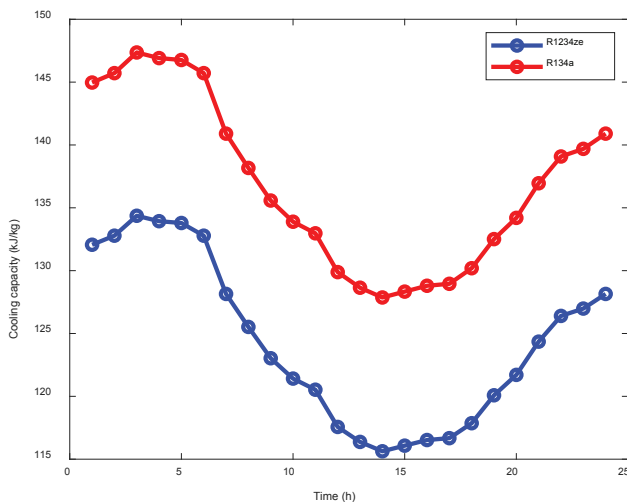


Figure 6. Hourly variation of cooling capacity (Ghardaia site).

Figure 7 illustrates the variation of the coefficient of performance (COP) for both refrigerants throughout the 21st day of July. The graph indicates that the COP of the R1234ze refrigerant surpasses that of R134a, given the specific evaporating and condensing temperatures. Moreover, the COP of R1234ze remains consistently above 4 throughout the entire 24-hour simulation period, demonstrating its superior performance within a broad operational range. For R1234ze, the COP of the VCR system fluctuates between 4.37 and 5.77, while for R134a, it ranges from 2.56 to 3.17. Therefore, the use of the refrigerant R1234ze(E) leads to an average increase of the COP value to 43.5%. The experimental works conducted by Leighton et al. [49] and Kabeel et al. [50] also shown the same trends as in the presented

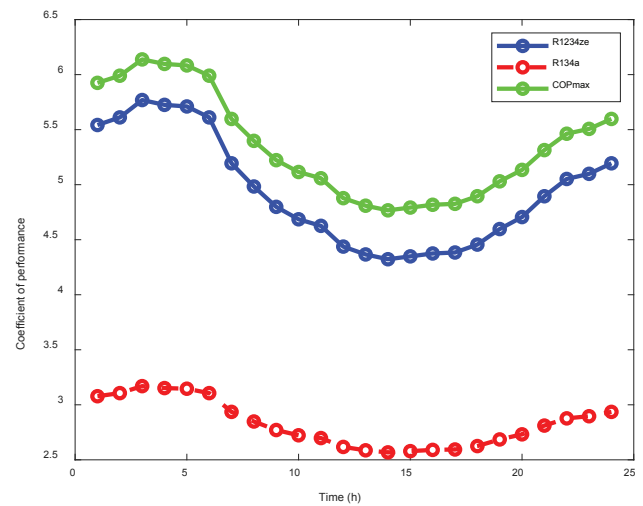


Figure 7. Hourly variation of coefficient of performance (Ghardaia region).

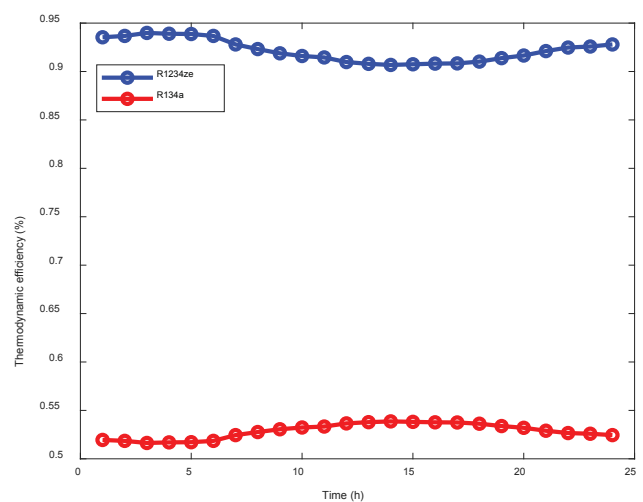


Figure 8. Hourly variation of thermodynamic efficiency (Ghardaia region).

work. They concluded that R1234ze has high COP by about 37.5% and 33%, respectively compared to R134a.

During the period from midnight to sunrise, the COP exhibits an increase due to the decrease in outside temperature, resulting in enhanced system performance. Conversely, as the atmospheric temperature rises, leading to higher condenser temperatures, the system's performance diminishes. Subsequently, from sunrise until around 14:00 PM, the COP experiences a decrease as the outside temperature gradually rises during this daytime period. However, the COP begins to rise again as the outside temperature decreases during the nighttime. It is worth noting that the COP values for R1234ze remain close to and exceed 90% of the maximum COP value, as depicted in Figure 8.

Figure 9 depicts the comparison of solar-to-cooling COP values for both refrigerants on the 21st day of July. It is evident that the solar-to-cooling efficiency of the VCR system tends to decrease as the ambient temperature rises. This decrease can be attributed to the decline in solar collector efficiency at higher temperatures, resulting in reduced conversion of solar energy into cooling output. The overall solar efficiency reaches its peak value around 03:00. Additionally, the VCR system's COP shows a downward trend at higher temperatures due to increased power consumption of the compressor and reduced refrigerant performance. The R1234ze refrigerant exhibits relatively favorable solar COP compared to R134a fluid. Between 10:00 and 19:00, the solar-to-cooling COP values range from 0.92 to 0.94. It is worth mentioning that currently available refrigeration systems typically have COP values ranging from 3 to 6 across standard operating temperature ranges, resulting in total solar-to-cooling COPs in the range of 0.3 to 0.6. However, the solar-to-cooling COP values for VCR

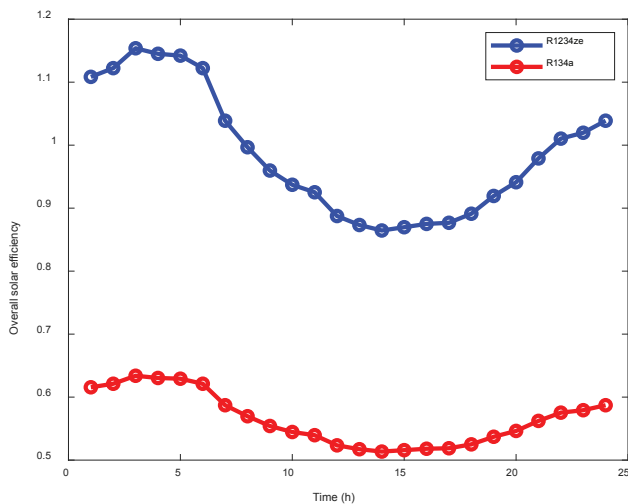


Figure 9. Hourly variation of overall solar efficiency (Ghardaia region).

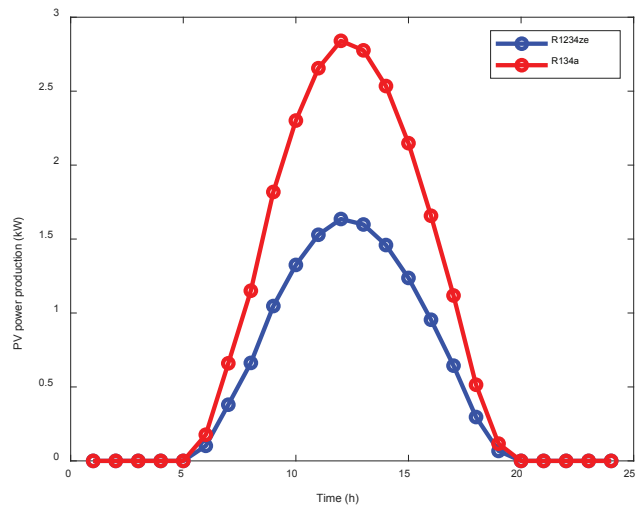


Figure 10. Hourly variation of PV power production (Ghardaia region).

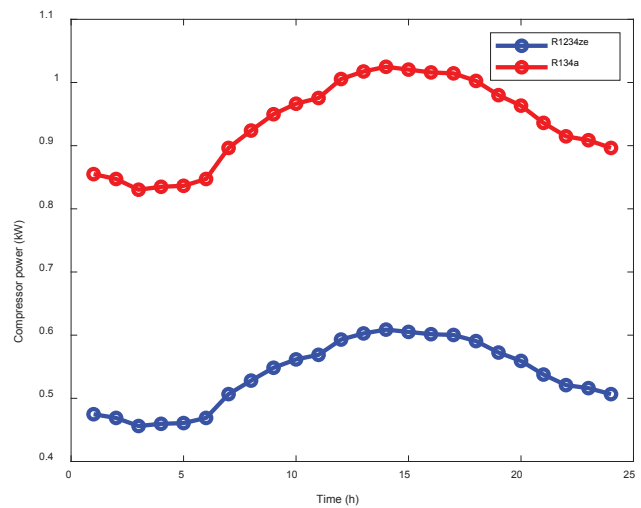


Figure 11. Hourly variation of compressor power (Ghardaia region).

systems can vary significantly depending on various factors, including solar collector efficiency, efficiency of electrical components (such as the compressor and fan), choice of refrigerant, and operating conditions.

Figure 10 presents the hourly variation of PV power production in terms of amount. Based on the results obtained for the 21st day of July, the highest PV power production for R134a and R1234ze refrigerants is observed at midday (12:00 PM) with values of 2.8 kWh and 1.6 kWh, respectively. The daily total power consumption of the compressor aligns with the daily total PV power production, as depicted in Figure 11. The compressor power consumption reaches its peak values between 14:00 PM and 18:00 PM when the atmospheric temperature and cooling load are at their maximum levels.

Conversely, the compressor power consumption gradually decreases during the morning and evening hours, corresponding to the decrease in atmospheric temperature. For the 21st day of July, the compressor power consumption ranges from 0.46 kW to 0.61 kW for R1234ze and from 0.83 kW to 1.02 kW for R134a. Thus, the compressor power consumption of R1234ze is 42.2 % lower than R134a. The obtained results are in accordance with the experimental data presented in [51–54].

The maximum compressor power consumption is observed at 14:00 PM. Consequently, the compressor power consumption increases in direct proportion to the atmospheric temperature and cooling load. Under these conditions, the compressor requires a higher driving power and may struggle to operate efficiently.

Figure 12 illustrates the hourly variation of the required PV panel area on July 21. It is evident that the PV surface area for both refrigerants exhibit an inverse relationship with ambient temperature, which is to be expected. Solar panels have a temperature coefficient, indicating the rate at which their efficiency decreases as temperature rises. As the temperature of the solar panels increases, their efficiency declines, resulting in reduced power generation for the same amount of sunlight. In hotter environments, the solar panels produce less power, necessitating an increase in the required panel area to compensate for this efficiency decrease.

Additionally, the required solar PV area for R134a refrigerant is higher compared to R1234ze fluid. This can be attributed to the larger quantity of R134a refrigerant needed to generate the same cooling effect as R1234ze. Consequently, a larger solar PV system is required to power the compressor responsible for circulating the refrigerant in the system. The larger system necessitates

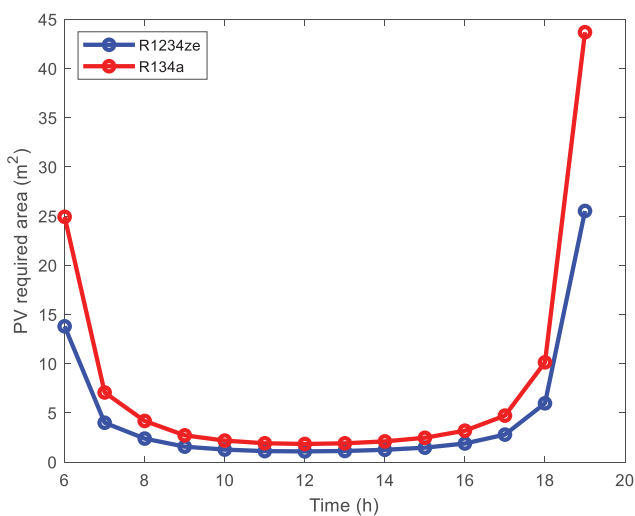


Figure 12. Hourly variation of PV required area (Ghardaia region).

more solar panels and, therefore, a larger surface area for capturing sunlight and generating electricity. However, it is worth noting that the PV panel surface area does not vary significantly with ambient temperature between 08:00 AM and 16:00 PM. This is because the power output of a PV panel primarily depends on the amount of solar radiation it receives rather than the ambient temperature. While temperature can impact panel efficiency, it does not directly influence the surface area required to generate a specific amount of power.

Figure 13 presents a comparison between the power consumed by the compressor and the power generated by PV panels on July 21st, utilizing R1234ze refrigerant at an evaporating temperature of 0°C. During the period of 7:00 PM to 6:00 AM, the PV panels generate a relatively low amount of power due to limited solar energy availability. Consequently, the energy demand cannot be fully met during this timeframe. However, from 8:00 AM to 16:00 PM, the PV panels produce more electricity than what the compressor motor requires. Any excess energy generated during this period is stored in an accumulator and utilized later to partially or entirely fulfill the compressor power demand between 19:00 PM and 6:00 AM.

According to Figure 14, the cumulative PV power production until 10:00 AM falls short of meeting the cumulative compressor power consumption. At 11:00 AM, the cumulative energy production and consumption become equal, and from that point onwards, the cumulative energy production surpasses the consumption, resulting in surplus solar-electricity being stored in the accumulators.

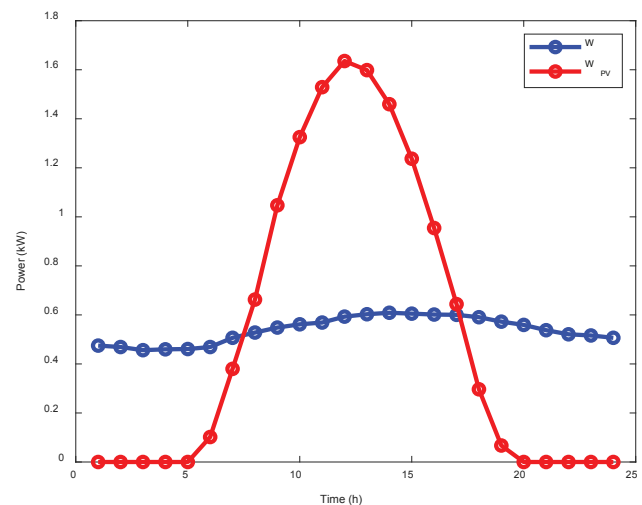


Figure 13. Comparison of the compressor power consumption and PV power production for R1234ze (Ghardaia region).

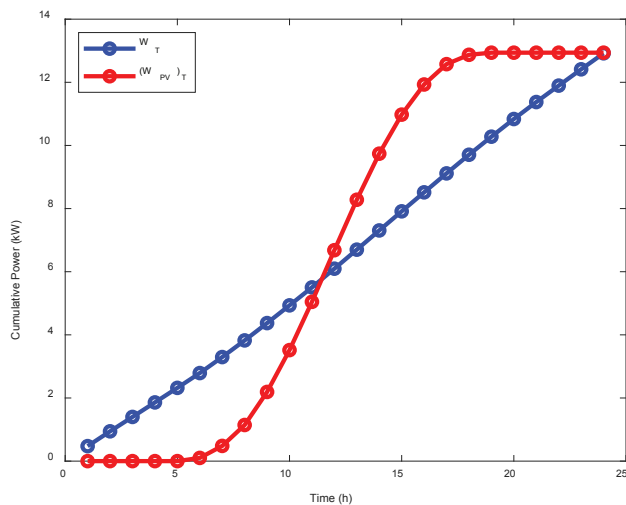


Figure 14. Comparison of the cumulative compressor power consumption and cumulative PV power production for R1234ze (Ghardaia region).

CONCLUSION

The growing demand for cooling applications and environmental concerns have spurred the development of solar-driven vapor compression refrigeration (VCR) systems with low GWP refrigerants. This study focuses on analyzing a solar-driven VCR system for cooling purposes in the Ghardaia region of Southern Algeria. The study compares the performance of R134a and its potential replacement, R1234ze, as working fluids. Key findings are as follows:

- In Ghardaia, the peak solar radiation occurs at 12:00 PM on July 21, reaching 2.726 kWh/m², with July generally experiencing higher radiation levels.
- At a given temperature, R134a requires a lower mass flow rate due to its higher enthalpy of vaporization. However, density becomes the dominant factor favoring a higher mass flow rate for R1234ze.
- R1234ze demonstrates a higher COP compared to R134a, thanks to its lower compressor power requirement and improved thermodynamic efficiency for the same cooling capacity.
- The solar-to-cooling COP declines as temperatures rise, primarily due to increased compressor power consumption and diminished refrigerant performance. Consequently, cooling capacity and efficiency are reduced.
- Although the required surface area of solar PV panels shows minimal variation with ambient temperature, panel temperature directly influences performance and, consequently, affects the required area.
- Cumulative PV power production exceeds compressor power consumption, indicating excess energy generation that can be stored for future use.

In conclusion, employing a solar-driven VCR system with low GWP refrigerants offers an energy-efficient and environmentally friendly cooling solution for the Ghardaia region. Utilizing R1234ze as the refrigerant significantly enhances system performance, resulting in noteworthy energy savings and cost reductions. Further research is necessary to assess the feasibility and scalability of implementing this system for commercial applications.

AUTHORSHIP CONTRIBUTIONS

Authors equally contributed to this work.

DATA AVAILABILITY STATEMENT

The authors confirm that the data that supports the findings of this study are available within the article. Raw data that support the finding of this study are available from the corresponding author, upon reasonable request.

CONFLICT OF INTEREST

The author declared no potential conflicts of interest with respect to the research, authorship, and/or publication of this article.

ETHICS

There are no ethical issues with the publication of this manuscript.

REFERENCES

- [1] Al-Yasiri Q, Szabó M, Arıcı M. A review on solar-powered cooling and air-conditioning systems for building applications. *Energy Rep* 2022;8:2888–2907. [\[CrossRef\]](#)
- [2] Ullah KR, Saidur R, Ping HW, Akikur RK, Shuvo NH. A review of solar thermal refrigeration and cooling methods. *Renew Sustain Energy Rev* 2013;24:499–513. [\[CrossRef\]](#)
- [3] Kaushik SC, Hans R, Manikandan S. Theoretical and experimental investigations on solar photovoltaic-driven thermoelectric cooler system for cold storage application. *Int J Environ Sci Dev* 2016;7. [\[CrossRef\]](#)
- [4] Alobaid M, Hughes B, Calautit J, O'Connor D, Heyes A. A review of solar-driven absorption cooling with photovoltaic thermal systems. *Renew Sustain Energy Rev* 2017;76:728–742. [\[CrossRef\]](#)
- [5] Kattakayam TA, Srinivasan K. Thermal performance characterization of a photovoltaic-driven domestic refrigerator. *Int J Refrig* 2000;23:190–196. [\[CrossRef\]](#)
- [6] Modi A, Chaudhuri A, Vijay B, Mathur J. Performance analysis of a solar photovoltaic-operated domestic refrigerator. *Appl Energy* 2009;86:2583–2591. [\[CrossRef\]](#)

- [7] Aktacir MA. Experimental study of a multi-purpose PV-refrigerator system. *Int J Phys Sci* 2011;6:746–757.
- [8] Ekren O, Yilanci A, Cetin E, Ozturk HK. Experimental performance evaluation of a PV-powered refrigeration system. *IEEE Elektron ir Elektrotech* 2011;114:7–10. [\[CrossRef\]](#)
- [9] Del Pero C, Butera FM, Buffoli M, Piegari L, Capolongo L, Fattore M. Feasibility study of a solar photovoltaic adaptable refrigeration kit for remote areas in developing countries. In *Proceedings of the 5th International Conference on Clean Electrical Power (ICCEP 2015)*. 2015:701–708. [\[CrossRef\]](#)
- [10] Kalbande SR, Deshmukh S. Photovoltaic Based Vapour Compression Refrigeration System for Vaccine Preservation. *Univ J Eng Sci* 2015;3:17–23. [\[CrossRef\]](#)
- [11] Kalbande SR, Deshmukh S, Khambalkar VP. Feasibility Evaluation of Solar Refrigeration System: A Case Study. *Int J Res Appl Nat Soc Sci (IMPACT: IJRANSS)*. 2016;4:87–94.
- [12] Li Y, Zhang G, Lv GZ, Zhang AN, Wang RZ. Performance study of a solar photovoltaic air conditioner in the hot summer and cold winter zone. *Sol Energy* 2015;117:167–179. [\[CrossRef\]](#)
- [13] Huang BJ, Hou TF, Hsu PC, Lin TH, Chen YT, Chen CW, et al. Design of direct solar PV-driven air conditioner. *Renew Energy* 2016;88:95–101. [\[CrossRef\]](#)
- [14] Li Y, Zhao BY, Zhao ZG, Taylor RA, Wang RZ. Performance study of a grid-connected photovoltaic-powered central air conditioner in the South China climate. *Renew Energy* 2017. [\[CrossRef\]](#)
- [15] Aguilar FJ, Aledo S, Quiles PV. Experimental analysis of an air conditioner powered by photovoltaic energy and supported by the grid. *Appl Therm Eng* 2017. [\[CrossRef\]](#)
- [16] Opoku R, Mensah-Darkwa K, Muntaka A. Techno-economic analysis of a hybrid solar PV grid-powered air-conditioner for daytime office use in hot humid climates - A case study in Kumasi city, Ghana. *Sol Energy* 2018;165:65–74. [\[CrossRef\]](#)
- [17] Opoku R, Anane S, Edwin IA, Adaramola MS, Seidu R. Comparative techno-economic assessment of a converted DC refrigerator and a conventional AC refrigerator both powered by solar PV. *Int J Refrig* 2016. [\[CrossRef\]](#)
- [18] Bilgili M. Hourly simulation and performance of solar electric-vapor compression refrigeration system. *Sol Energy* 2011;85:2720–2731. [\[CrossRef\]](#)
- [19] Mba EF, Chukwunke JL, Achebe CH, Okolie PC. Modeling and simulation of a photovoltaic powered vapor compression refrigeration system. *J Inf Eng Appl* 2012;2:1–15.
- [20] Gupta BL, Bhatnagar M, Mathur J. Optimum sizing of PV panel, battery capacity and insulation thickness for a photovoltaic operated domestic refrigerator. *Sustain Energy Technol Assess* 2014;7:55–67. [\[CrossRef\]](#)
- [21] Torres-Toledo V, Meissner K, Coronas A, Müller J. Performance characterization of a small milk cooling system with ice storage for PV applications. *Int J Refrig* 2017.
- [22] Sharma NK, Singh H, Sharma MK, Gupta BL. Performance analysis of vapour compression and vapour absorption refrigeration units working on photovoltaic power supply. *Int J Renew Energy Res* 2016;6:455–464.
- [23] Hammad M, Tarawneh T. Performance study of a DC refrigerator powered by solar PV modular sets: paper II. *J Dyn Mach* 2018;1:1–11. [\[CrossRef\]](#)
- [24] Salilih EM, Birhane YT. Modelling and performance analysis of directly coupled vapor compression refrigeration solar refrigeration system. *Sol Energy* 2019;190:228–238. [\[CrossRef\]](#)
- [25] Su P, Ji J, Cai J, Gao Y, Han K. Dynamic simulation and experimental study of a variable speed photovoltaic DC refrigerator. *Renew Energy* 2020;152:155–164. [\[CrossRef\]](#)
- [26] Gao Y, Ji J, Han K, Zhang F. Comparative analysis on performance of PV direct-driven refrigeration system under two control methods. *Int J Refrig* 2021;127:21–33. [\[CrossRef\]](#)
- [27] Mota-Babiloni A, Makhnatch P, Khodabandeh R. Recent investigations in HFCs substitution with lower GWP synthetic alternatives: Focus on energetic performance and environmental impact. *Int J Refrig* 2017;82:288–301. [\[CrossRef\]](#)
- [28] Ben Jemaa R, Mansouri R, Boukholda I, Bellagi A. Energy and Exergy Investigation of R1234ze as R134a Replacement in Vapor Compression Chillers. *Int J Hydrogen Energy* 2016;1–11. [\[CrossRef\]](#)
- [29] Rajendran P, Sidney S, Ramakrishnan I, Dhasan ML. Experimental studies on the performance of mobile air conditioning system using environmental friendly HFO 1234yf as a refrigerant. *Proc Inst Mech Eng Part E J Process Mech Eng* 2019. [\[CrossRef\]](#)
- [30] Touaibi R, Koten H. Energy Analysis of Vapor Compression Refrigeration Cycle Using a New Generation Refrigerants with Low Global Warming Potential. *J Adv Res Fluid Mech Therm Sci* 2021;87:106–117. [\[CrossRef\]](#)
- [31] Prasad US, Mishra RS, Das RK, Soni H. Experimental and Simulation Study of the Latest HFC/HFO and Blend of Refrigerants in Vapour Compression Refrigeration System as an Alternative of R134a. *Processes* 2023;11:814. [\[CrossRef\]](#)
- [32] Zaghba L, Khennane M, Fezzani A, Borni A, Hadj Mahammed I. Experimental performance assessment of a 2.25 kWp Rooftop PV system installed in the desert environment: a case study of Ghardaia, Algeria. *Int J Sustain Eng* 2020. [\[CrossRef\]](#)
- [33] Kyoto Protocol. Report of the Conference of the Parties, United Nations Framework Convention on Climate Change (UNFCCC). 1997.

- [34] Directive 2006/40/EC of the European Parliament and of the Council of 17 May 2006 Relating to Emissions from Air Conditioning Systems in Motor Vehicles and Amending Council Directive 70/156/EC. Off J Eur Union. 2006.
- [35] Regulation (EU) No 517/2014 of the European Parliament and the Council of 16 April 2014 on Fluorinated Greenhouse Gases and Repealing Regulation (EC) No 842/2006. Off J Eur Union. 2014.
- [36] Hodnebrog Ø, Etminan M, Fuglestedt JS, Marston G, Myhre G, Nielsen CJ, Shine KP, Wallington TJ. Global warming potentials and radiative efficiencies of halocarbons and related compounds: A comprehensive review. *Rev Geophys*. 2013;51:300–378. [\[CrossRef\]](#)
- [37] Censi G, Padovan A. R1234ze(E) as drop-in replacement for R134a in a micro-fin shell-and-tube evaporator: Experimental tests and calculation model. In *Proceedings of the 18th International Refrigeration and Air Conditioning Conference*, West Lafayette, IN, USA, 24-28 May 2021.
- [38] Hartmann DL, Klein Tank AMG, Rusticucci M, Alexander LV, Brönnimann S, Charabi Y, et al. Observations: Atmosphere and Surface. In: Stocker TF, Qin D, Plattner G-K, Tignor M, Allen SK, Boschung J, Nauels A, Xia Y, Bex V, Midgley PM, eds. *Climate Change 2013: The Physical Science Basis*. Cambridge University Press; 2013:p.159–254. [\[CrossRef\]](#)
- [39] Lemmon EW, Huber ML, McLinden MO. REFPROP, NIST Standard Reference. 2014.
- [40] Moran MJ, Shapiro HN. *Fundamentals of Engineering Thermodynamics*, fifth ed. John Wiley and Sons Inc; 2006.
- [41] Yamankaradeniz R, Horuz I, Kaynakli O, Coskun S, Yamankaradeniz N. *Refrigeration Techniques and Heat Pump Applications*, second ed. Dora Company; 2009. ISBN: 978-605-4118-14-4.
- [42] Bahadori A. Chapter 5 - Gas Compressors in Natural Gas Processing. Gulf Professional Publishing; 2014. pp. 223–273. [\[CrossRef\]](#)
- [43] Kourchi M, Rachdy A. Calcul Rapide des Propriétés Thermodynamiques des Frigorigènes [Fast Calculation of Thermodynamic Properties of Refrigerants]. *Int J Innov Appl Stud*. 2016;14.
- [44] Życzkowski P, Borowski M, Łuczak R, Kuczera Z, Ptaszyński B. Functional Equations for Calculating the Properties of Low-GWP R1234ze(E) Refrigerant. *Energies*. 2020;13:3052. [\[CrossRef\]](#)
- [45] Kim DS, Infante-Ferreira CA. Solar refrigeration options - state-of-the-art review. *Int J Refrig*. 2008;31:3–15. [\[CrossRef\]](#)
- [46] Sánchez D, Cabello R, Llopis R, Arauzo I, Catalán-Gil J, Torrella E. Energy performance evaluation of R1234yf, R1234ze(E), R600a, R290 and R152a as low-GWP R134a alternatives. *Int J Refrig*. 2017;74:267–280. [\[CrossRef\]](#)
- [47] Mota-Babiloni A, Navarro-Esbrí J, Barragán A, Molés F, Peris B. Drop-in energy performance evaluation of R1234yf and R1234ze(E) in a vapor compression system as R134a replacements. *Appl Therm Eng*. 2014;71:259–265. [\[CrossRef\]](#)
- [48] Colombo LPM, Lucchini A, Molinaroli L. Experimental analysis of the use of R1234yf and R1234ze(E) as drop-in alternatives of R134a in a water-to-water heat pump. *Int J Refrig*. 2020;115:18–27. [\[CrossRef\]](#)
- [49] Leighton D, Hwang Y, Radermacher R. Modeling of household refrigerator performance with low global warming potential alternative refrigerants. *ASHRAE Trans*. 2012;118:658–665.
- [50] Kabeel AE, Khalil A, Bassuoni MM, Raslan MS. Comparative experimental study of low GWP alternative for R134a in a walk-in cold room. *Int J Refrig*. 2016;69:303–312. [\[CrossRef\]](#)
- [51] Mendoza-Miranda JM, Mota-Babiloni A, Navarro-Esbrí J. Evaluation of R448A and R450A as low-GWP alternatives for R404A and R134a using a micro-fin tube evaporator model. *Appl Therm Eng*. 2016;98:330–339. [\[CrossRef\]](#)
- [52] Molinaroli L, Lucchini A, Colombo LPM. Experimental comparison of the use of R134a and R1234ze(E) in a semi-hermetic reciprocating compressor. *Proceedings of the 25th IIR International Congress of Refrigeration: Montréal, Canada, August 24-30, 2019*.
- [53] Ramírez-Hernández HG, Morales-Fuentes A, Sanchez-Cruz FA, Méndez-Díaz S, García-Lara HD, Martínez-Martínez S. Experimental study on the operating characteristics of a display refrigerator phasing out R134a to R1234ze(E) and its binary blends. *Int J Refrig*. 2022;138:1–12. [\[CrossRef\]](#)
- [54] Conte R, Azzolin M, Bernardinello S, Del Col D. Experimental investigation of large scroll compressors working with six low-GWP refrigerants. *Therm Sci Eng Prog*. 2023;44:102043. [\[CrossRef\]](#)